Unsupervised Learning of Signal Strength Models for Device-Free Localization

Amal Al-Husseiny
Computer and Systems Engineering Department
Mansoura University, Egypt
Email: amal_lotfy@mans.edu.eg

Neal Patwari
McKelvey School of Engineering
Washington University in St. Louis
Email: npatwari@wustl.edu

***Abstract*—RSS-based device-free localization (DFL) systems make use of the received signal strength (RSS) changes in a network of static wireless nodes to locate and track people. Current DFL systems require calibration, which depending on the method and required accuracy, can be very expensive in terms of time and effort, making DFL system deployment and maintenance challenging. This paper implements unsupervised learning of signal strength models (UnLeSS), a Baum-Welch based method to learn the parameters of a hidden Markov model (HMM) for each link, including the RSS distribution during the no-crossing state and the crossing state. The system uses the HMM to estimate the probability of each link being in the crossed state. As a demonstration of its effectiveness, the per-link probability is used in a radio tomographic imaging algorithm to track the location of a person. Experiments are conducted in two different homes to determine the performance of UnLeSS. We demonstrate that our system is capable of estimating the crossing/no-crossing distribution with Kullback-Leibler divergence maximum of 1.43. UnLeSS is capable of tracking a person with high accuracy (0.66 m) without a calibration period.**

I. Introduction

Device-free localization (DFL) using radio frequency (RF) sensing has many useful applications. Device-free localization (DFL) is very valuable for many applications from tracking [11], [9], [23], [16] and ambient assisted living [1] to security and border protection [2]. For example, in ambient assisted living, people may not be able or willing to always carry a device that locates them. All DFL methods have accuracy that degrades over time due to environmental changes which cause the collected calibration information or fingerprint map to deviate from the actual state of the network. This paper provides a method to keep track of the statistical models of RSS without active calibration or labelling from the user, even as the environment changes.

UnLeSS is a device free localization system that is capable of adapting to environmental changes by updating the RSS distributions' parameters (means and variances for the distributions when a link is crossed and not crossed). Such a system is more applicable to real-world environments in which changes occur rapidly and frequently, causing current DFL methods' performance to degrade over time. Ambient assisted living as an example application will benefit from UnLeSS — many methods require frequent and extended periods of time when no person is present — assisted living residents tend to be present all day, and it would not be acceptable to ask them to leave just to recalibrate a DFL system. In this paper, we build and test a system running UnLeSS using radio tomographic imaging (RTI) on two datasets collected from RF sensor networks deployed in two homes. We use the datasets to quantify the performance of the proposed methods, including the accuracy of the estimated link statistical RSS models, the accuracy of line crossing detectors and the localization algorithms which use the models.

Current DFL methods fall into two categories: 1) fingerprinting, and 2) model-based. All RF-based DFL methods, either fingerprint-based or model-based, are actually based on some model, whether it is a measurement-based model or an *a priori* statistical model. The actual RSS measurements on each link change with time, causing performance to degrade. Fingerprint methods [16], [20] require time consuming and tedious collection of channel measurements labelled with the current location of the person, for each of the many possible locations within the coverage area. Fingerprint methods are highly accurate at the start, and accuracy degrades exponentially as changes are made to the environment [8]. Model-based methods require a single fingerprint of the empty area, the coordinates of the nodes, and an *a priori* model for the statistical channel changes measured when a person is near a link, as a function of the transmitter, receiver, and person locations. The model is assumed to hold for every link in the network, and the parameters of this model need to be determined *a priori*. Due to the loss in accuracy from the generalization and the assumed model parameters, a model-based method's accuracy is initially lower than a fingerprint method.

Despite the importance of DFL, the state-of-the-art still is unable to combine high-accuracy localization, ease of setup, and consistent performance over time. In this paper we develop methods to automatically learn the statistical RSS model from unlabelled measurement data. We develop and test methods to train a hidden Markov model (HMM). From these methods, we can estimate the distributions of RSS in two states:

1) *Crossing state*: A person is present on or near the link line (the imaginary line connecting transmitter and receiver for a link)
2) *No-crossing state*: No person is present anywhere near the link line.

978-1-7281-0270-2/19/$31.00

We call these two distributions the link's statistical RSS model. Automatic learning of the statistical RSS models for all links in the network is one critical part of consistently achieving the high accuracy possible from fingerprinting methods without collecting location-labelled training data. The performance of the HMM-based unsupervised learning method is shown to be better than other tested unsupervised learning models.

Next, using the statistical RSS models in a HMM, we estimate the probability of each state (crossing or no-crossing) over time using the forward algorithm [15]. We explore the performance of using these forward probabilities as input to a radio tomographic imaging (RTI) algorithm to estimate an image map of the people present in the area of interest. Such system is able to learn and improve the localization output over time without the need for repeated collection of a fingerprint database. In this paper, we do not study adaptively setting each link's *spatial model* [6], that is, the area in which a link's RSS is sensitive to a person's presence, however, such efforts are complementary to the statistical RSS model studied here.

We show that the DFL based on UnLeSS reduces localization error by 40% compared to multi-channel attenuation based RTI [5] and by 20% compared to an X-means clustering technique [12] combined with the same forward algorithm.

The rest of this paper is organized as follows. Section II presents the system design and introduces the methodology. Sections III-A, III-B and III-C describe in detail the main components of UnLeSS system. The system evaluation is presented in Section V in which the localization accuracy of the proposed system is quantified. We describe related research in Section VI. Then, we conclude and talk about future work in Section VII.

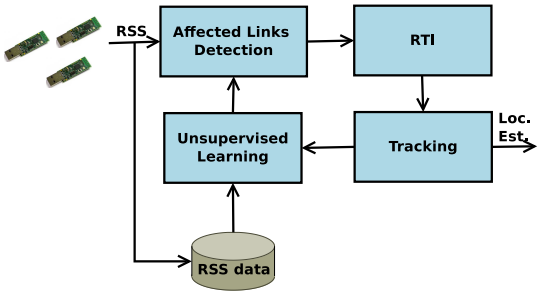

Fig. 1: System Block Diagram

II. System Design

In this section, we introduce the proposed unsupervised learning of signal strength models (UnLeSS) localization system components as shown in the system block diagram in Figure 1. The UnLeSS system uses RF sensors deployed within the area of interest to take RSS measurements on multiple channels between multiple pairs of RF transceivers in order to estimate the locations of persons in the deployment area. We use $r_{l,c}(t)$ to denote an RSS measurement in dBm on link l, channel c, and at time t. The time series of recent RSS measurements for a link and channel are stored for use by an unsupervised learning algorithm (e.g., the Baum-Welch algorithm) which estimates the link's statistical RSS model.

Next, in the *affected links detection module*, the estimated models are used to generate the probabilities that link l is affected at time t. These probabilities, α, are then used as a measurement vector input to the RTI module. The RTI module estimates an image map $\hat{x}$ which quantifies presence per voxel in the area of coverage. Whenever the maximum image intensity is higher than a threshold, the system assumes a person is present. We evaluate localization of a single person, and thus in this paper, we estimate location using the coordinates of the voxel with the maximum value. The unsupervised learning can be scheduled to run periodically to ensure the model parameters are updated as the environment changes over time.

We assume that the distributions of RSS in the crossing and no-crossing states are different and that the conditional distributions for both states are Gaussian. We also assume that the random process of crossing/no-crossing for each link is a Markov process and independent of other links.

Although in model-based DFL we really want to know whether a person is crossing the link line or not, in reality, all we can obtain from the RSS measurements is really whether or not the link's RSS distribution is affected by the presence of a person or not. This is one of the challenges of this paper, and any paper that uses a geometric model to infer location from RSS measurements. We address this challenge by evaluating the UnLeSS method for its ability to accurately predict the distribution of RSS parameters in two dichotomies: first the "crossing / no crossing" dichotomy defined by a person being in the narrow ellipse around the line line or not; and second the "affected / not affected" dichotomy defined by a person being in any location which significantly changes the RSS or not. The first is important for geometric model-based DFL, and the second is important for other applications including machine learning-based methods. By evaluating both, we explicitly consider the impact of UnLeSS in both cases.

III. Methods

A. Unsupervised Learning for Link RSS

In this section, we describe the particular challenges of unsupervised learning of RSS distributions. In general, unsupervised learning is challenging and can lead to unpredictable modeling outcomes. We take advantage of a few particular characteristics of RSS and the nature of motion in an environment in order to ensure that the learned parameters are reliable and close to the ground truth. In the UnLeSS algorithm, we modify a Baum-Welch algorithm with constraints to meet our particular goals. We first describe the motivations for the modifications and then show that they improve results.

Each link line at a particular time can be in one of two states, crossing or no-crossing by the existence of the person being localized. Generally, the crossing state has a higher RSS variance than the no-crossing state. The crossing state's RSS mean also changes from the no-crossing state's RSS mean. Since the human motion is slow compared to the measurement

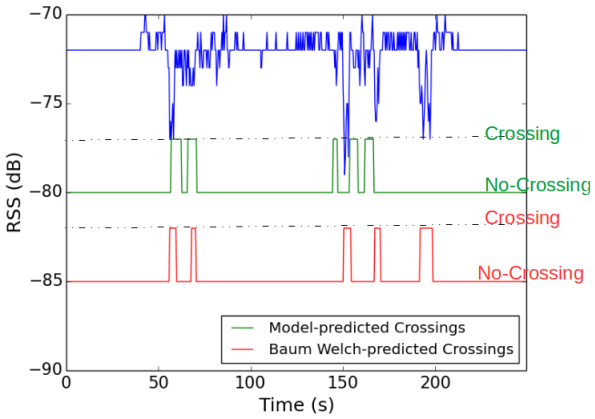

Fig. 2: RSS for one of the links with highlighted crossing periods for both the modeled predicted and the UnLeSS predicted crossings while imposing constraints on the transition probabilities.

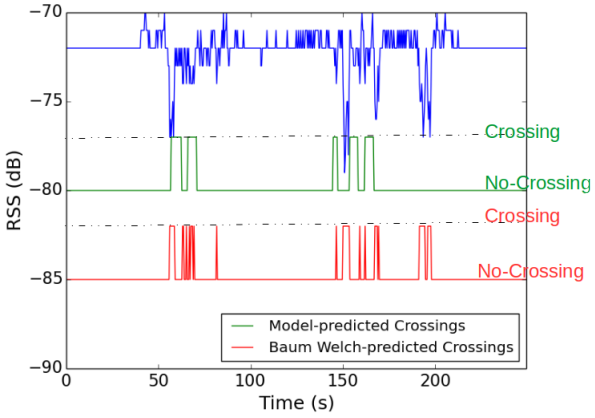

Fig. 3: RSS for one of the links with highlighted crossing periods for both the modeled predicted and the UnLeSS predicted crossings without any constraints on the transition probabilities. The crossing states for both are given probability of 1 and the no-crossing a probability of 0.

sampling rate, the transitions from one state to the other is predicted to be rare.

As described in the Introduction, each link has $N = 2$ states, the crossing state, S_0, and the no-crossing state, S_1. The goal of the unsupervised learning algorithm in UnLeSS is to use a sequence of RSS observations $O_{l,c} = [r_{l,c}(1), \ldots, r_{l,c}(T)]^T$ to estimate the conditional probability distributions $b_i = P[r_{l,c} = r \,|\, S_i]$. This can be achieved using Baum Welch unsupervised training method [14].

Unsupervised learning of the models b_i, $i = \{0, 1\}$ can have an overfitting problem if too many model parameters need to be determined. We choose to model RSS in dB as Gaussian distributed in order to match measurements as close as possible without increasing the number of model parameters beyond two. There is analytical support for a Gaussian distribution in the no-crossing state [21]. When many links RSS data in state i are considered together as in [19], a skew-Laplace distribution fits well; however, this may be because each link's $P[r_{l,c} = r \,|\, S_0]$ has a different mean and variance and the mixture of these models is approximately skew-Laplace.

With the Gaussian approximation, the UnLeSS algorithm must estimate four parameters for each link, the mean μ_i and variance U_i for states $i = 0, 1$. A Markov model also has a state transition probability matrix A and initial probability distribution π. We also note that we use the generalized continuous-valued version of the hidden Markov model in which each observation is a continuous random variable $r_{l,c}$.

Without constraints, an unsupervised learning algorithm, i.e., Baum Welch algorithm, has no particular method to ensure that the "crossing" state has a higher variance of RSS, and is usually experienced for a shorter time than the "no-crossing" state. Our algorithm uses two constraints to ensure that the two learned distributions converge correctly.

First, the Baum-Welsh algorithm is iterative and requires an initial guess. We initialized π and A as $\pi_0 = 0.001, \pi_1 = 0.999$ and for $A_{00}, A_{01}, A_{10}, A_{11}$ the values $0.98, 0.02, 0.001, 0.999$ respectively.

We initialize b_i, the conditional distribution of the RSS, as follows. Let $\tilde{\mu}$ and $\tilde{U}$ be the average and standard deviation of RSS across the initial data set. We initialize $\mu_1 = \tilde{\mu}$, $\mu_0 = \tilde{\mu} - 7$ dBm because we know the mean RSS tends to decrease, on average, on links that a person obstructs. We initialize the $U_1^2 = \tilde{U}^2$ and $U_0^2 = 3.0\tilde{U}^2$ because we know that the RSS variance increases when a person is moving near the link line. Both settings also tend to enforce that the state S_1 should have higher mean and lower variance of RSS. These are settings which have been used in prior RF sensing work when model learning was performed [2].

This initialization encourages the model to converge to a low probability of being in S_0, the crossing state, and the very high probability of staying in the S_1 state. Second, in order to ensure that our unsupervised learning method transitions between states as rarely as happens in real life, we upper bound A_{00} and A_{11}. We ensure $A_{01} < 0.02$ and $A_{10} < 0.001$ by limiting their estimate. We, also, ensure the state with the higher RSS variance gets assigned to the crossing state.

The advantage of using such an unsupervised training algorithm is that there is no need to tune training parameters or provide feedback about the user's actual location. Also, the system has the capability to be updated automatically in case the environment changes after setup, i.e., furniture moves.

The Baum-Welch training, while computationally expensive, is not required to be re-run with each new sample. We assume it is re-run each T samples, and study the performance of UnLeSS as a function of T.

As some of the link lines are never crossed (for example, if two nodes are on the same wall), there may be links which, in reality, have only one cluster, namely the no-crossing cluster. To compare the performance of Baum-Welch learning algorithm with other unsupervised learning algorithms, we used X-means. X-means is a K-means clustering technique

that outputs both the number of clusters and their parameters. It is much faster than repeatedly running K-means for different values of K [12]. X-means is used to cluster the RSS for each time stamp into a crossing or no-crossing clusters, then the mean and variance for each state are estimated and used as the model parameters for the HMMs for the different links. The probabilities of each link being crossed or not are then fed into the RTI localization module.

B. Affected Links Detection

The goal of the affected links detection module in UnLeSS system is to automatically identify whether the links under question are affected or unaffected by the existence of a person in the area of interest at each point of time. To do this, we use unsupervised learning, comparing algorithms based on the HMM developed in Section III-A and a baseline X-means method. From the probability models trained using Baum-Welch algorithm on past data, we use the forward algorithm to compute, at each time t, the probability of link l being affected by the existence of a person given the RSS measurements collected up to time t.

As can be seen from Figure 2, the periods of time the shown link RSS is affected by the existence of a person within the area of interest can be identified by eye. For the shown link in Figure 2, the person can be seen to have affected that link between the time pairs (53,58), (149,153), (166,170) and (189,198). To evaluate the trained HMM and its accuracy estimating the crossing/no-crossing state, we need to predict the actual crossing/no-crossing state for each time clock t in the time sequence T for our two deployments. To assign a state for each time t for each link line, we estimated whether the actual person position coordinates, recorded during the measurements collection, is within an ellipse whose focal points are the transceivers forming the link line under question. When the coordinates of the moving person is within the ellipse, then the link line is in a crossing state, otherwise, the link line is in a no-crossing state. We call this the model-predicted states.

After assigning a state (crossing/no-crossing) for each time t for each link line, we, then, calculate the mean and variance of all the timestamps with a crossing state for each link line and consider those as the mean and variance of the crossing state, respectively, for the crossing state of each link line. We also calculate the mean and variance of all the RSS measurements with timestamps with a no-crossing state for each link line and consider those as the mean and variance of the no-crossing state, respectively, for the no-crossing state of each link line.

Using the state assignments and the estimated mean and variance for both states for each link line, we can evaluate the accuracy of the trained HMMs and their state predictions. To confirm that the Baum-Welch forward probabilities for affected links detection do predict the actual state and for that reason deviate from the model predicted states, we plotted RSS for each link l and channel $c \in C$ and highlighted the crossing periods according to the ellipse model prediction and the Baum Welch training and forward probabilities prediction. Figure 2 shows a sample of these plots. We can see that the Baum Welch state prediction while it deviates from the ellipse model prediction, it can accurately predict the periods where the RSS changes indicating the presence of a person in the area of effect. The logic behind that can be explained looking

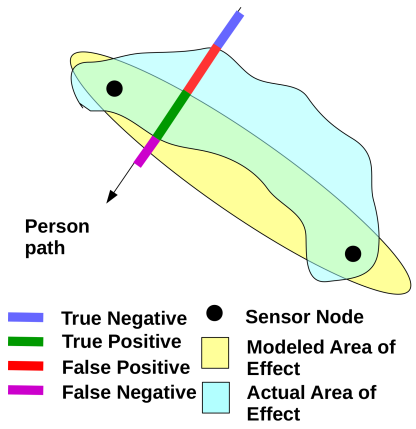

Fig. 4: When an elliptical model is used for the "ground truth" for link presence, and the RSS is actually affected within a different area, the detector is evaluated to have false positives and negatives even if it perfectly detects the true period in which the RSS is affected.

at Figure 4. We can see that while the modeled area of effect between two sensor nodes is a neatly shaped ellipse, the actual area of effect deviates from the ellipse shape resulting in areas where comparing to the model predicted state will lead to a false positive (FP) or false negative (FN) cases while in actuality comparing to the actual state, it should be considered true positive (TP) and true negative (TN) cases respectively.

To ensure the accuracy of the model-predicted states, we randomly selected 50 links from the links of both our two deployment. For those randomly selected links, we plotted the RSS vs. time as in Figure 5 and then, we manually annotated each crossing interval as being in the crossing state and the rest as no-crossing state. after that, we compared the manual states assignment to the modeled states prediction. We, also, compared the manual states mean and variance to the model predicted states mean and variance.

C. Localization

In this section, we summarize the RTI method used to process the RSS measurements collected and localize the person being tracked in the both our deployments and presented in [17].

An RTI system is composed of N RF-sensors communicating at C different frequency channels. These sensors are deployed at known positions, $\mathbf{z}_n, n = 1, \ldots, N$. At each time instant t, the system measures the RSS $r_{l,c}$ for each link l and channel $c \in C$.

The collected RSS measurements from all the links $l \leq N(N-1)$ in the network and on all the C selected frequency

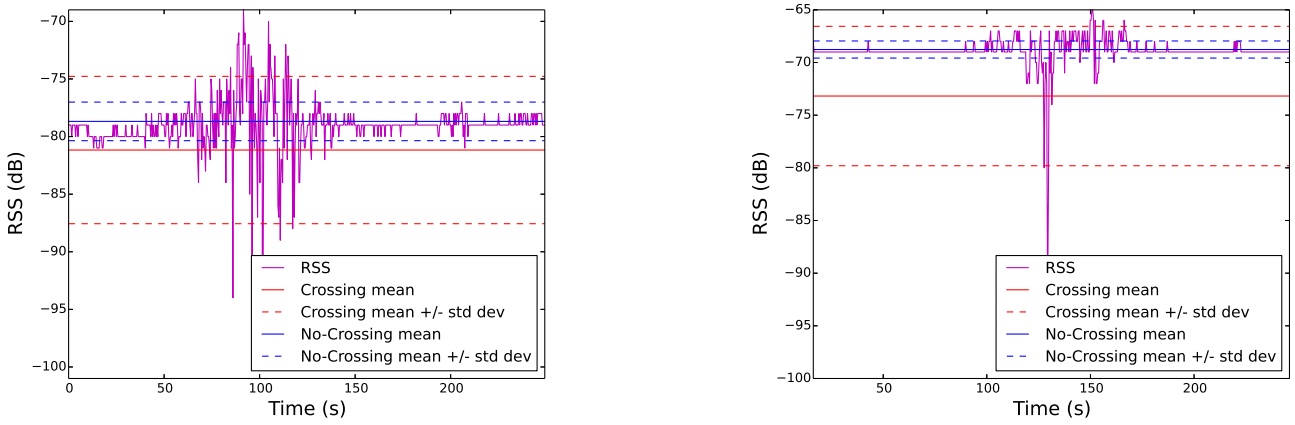

(a) (b)

Fig. 5: RSS measurements, UnLeSS generated mean and mean +/- standard deviation for both the crossing and the no-crossing states for links a) (Tx=0, Rx=4, ch=2) Deployment I b) (Tx=0, Rx=4, ch=0) Deployment II

channels are combined to estimate the change in the propagation field caused by the existence of people in the area of interest being monitored.

In RTI, the deployment field is discretized into voxels. When all the L links of the network are considered, the changes in the propagation field of the monitored area can be estimated as:

$$y = Wx + n \tag{1}$$

where y is the measurements vector, which in our case is the forward probability for each link l, n is the noise vector and x is the image to be estimated.

The model for RTI, (1) models the relationship between the image x and the forward probabilities y as a linear relationship. In general, RTI models are approximations of the complicated multipath radio propagation equations. This paper does introduce an additional approximation since the forward probabilities y are constrained to values $\in [0, 1]$. Future work should evaluate methods to improve linearity when there are multiple people in the area of interest. In this paper, we evaluate UnLeSS for experiments with only one person present in the area of interest.

IV. Experimental Setup

A. Measurement Collection

For the sake our evaluating UnLeSS, we performed two deployments, Deployment I and Deployment II. In Deployment I, we deployed a $N = 30$ RF sensor network on one floor of single family house while in Deployment II, we deployed a $N = 27$ RF sensor network, also, on one floor of a single-family house. Sensors were placed on tables, window sills, and furniture, at a range of heights from 0.3 to 1.0 m. In both deployments, the house is furnished as arranged by its residents, and the natural state of the environment was not modified for our experiments. Deployment I area is approximately rectangular, 11 m by 10 m, including a kitchen, dining room, living room, entrance, hallway, bathroom, and bedroom. Deployment II is, also, approximately rectangular, 11 m by 12 m, including a kitchen, living room, entrance, hallway, bathroom, and three bedrooms.

The sensors composing the network are Texas Instruments CC2531 USB dongles which are 2.4-GHz IEEE 802.15.4-compliant transceivers [3]. The sensors are set to have 4.5 dBm transmit power and run a multi-channel token passing protocol, multi-Spin, in which the sensors transmit in TDMA fashion with a sequence defined by their ID. If not transmitting, the sensors are in receiving mode [1], [4].

Each packet contains the transmitting node ID and the most recent RSS measurements of the packets received from other sensors. If a packet is dropped, after a back-off time, the next sensor in the schedule transmits which makes the network tolerant to packet drops. At the end of each communication cycle, the sensors switch synchronously to the next frequency channel found in a pre-defined list. On average, the time interval between two consecutive transmissions is 2.9 ms [1], [4].

The calibration measurements were taken while the environment was vacant. The calibration stage lasted for around 12 seconds for both Deployments. The RSS measurements from the calibration stage for each link and channel pair are then averaged to determine $\bar{r}_{l,c}$ to be used for comparison with the attenuation-based RTI algorithm.

V. Evaluation

This section presents results from our proposed methods.

A. Mean and Variance Estimation

We first evaluate the accuracy of UnLeSS estimated mean $\bar{\mu}$ and variance $\bar{U}$ for each link l and channel $c \in C$. To do so, we compare our UnLeSS generated mean, $\bar{\mu}_{l_c}$, and variance $\bar{U}_{l_c}$ for both the crossing and the no-crossing states to model generated mean and variance for each link l and channel

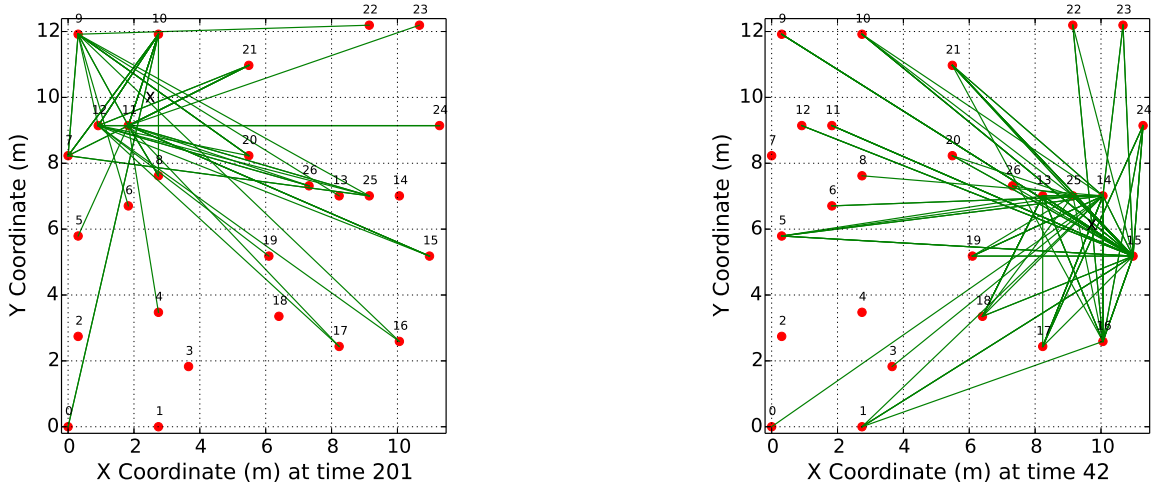

(a) (b)

Fig. 6: Affected links (—), sensors (●) actual position of the person (X) at two different times.

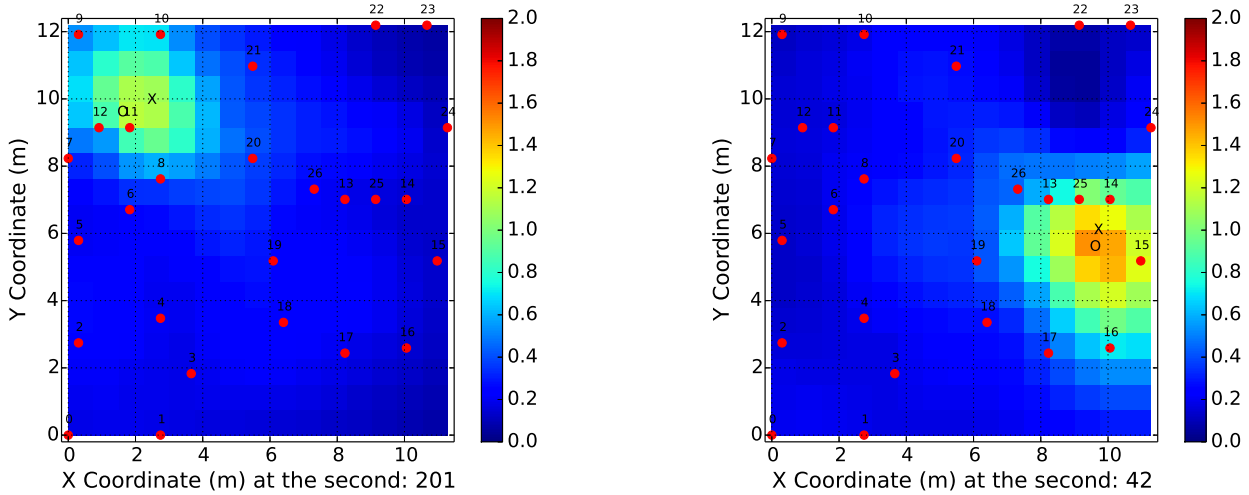

(a) (b)

Fig. 7: The radio tomographic image with sensors (●), actual position of the person (X), estimated position of the person (O) at two different times.

	vs. Model		vs. Human	
	Crossing	No-Crossing	Crossing	No-Crossing
UnLeSS	1.095	565	0.730	0.350
SSBCL	9.600	4.505		
X-means	4.130	0.340	2.330	0.475
Model			1.960	0.460

TABLE I: Kullback-Leibler divergence between RSS distributions generated by elliptical model (Model) and those generated from: UnLeSS, signal strength-based boundary crossing localization [13] (SSBCL), and X-means for two deployments.

$c \in C$. Figure 5 shows RSS measurements, UnLeSS generated mean and mean plus or minus one standard deviation for both the crossing and the no crossing states for two example links. We can see from the plots that the generated mean and variance are good estimates for the real mean and variance for both the crossing and the no crossing states for these two links. Generally, most links follow our intuitive understanding of what the mean and variance should be for the two states. We also compared the model generated mean and variance for each link l and channel $c \in C$ to the mean and variance generated using the model presented in [13] and using X-means clustering [12]. Table I summarizes the root mean square of Kullback-Leibler divergence computed for each link l and channel $c \in C$ assuming Gaussian distribution and using the model computed mean and variance as the true distribution.

We can see that for both deployments, Deployment I and Deployment II, the UnLeSS generated crossing state distribution has the lowest Kullback-Leibler divergence and hence is a better estimate than other methods. For the no-crossing state X-means generated a better fit distribution, but the crossing states exhibit significantly higher divergence than UnLeSS.

As we noted, the elliptic model for assigning crossing/no-crossing states is not always accurate, and we also need to quantitatively validate that the proposed algorithm performs well at identifying periods when we can see that the RSS is affected, not simply those times when the person is in the link's ellipse. We manually annotated state, by looking only at the link's RSS data, to fifty links from each deployment at each time t. We use our manual state labels to calculate the mean and variance for both the crossing and no-crossing distributions. We compared the manually generated crossing and no-crossing distributions for each of the fifty links to the crossing and no-crossing distributions generated using the model presented in [13] and using X-means clustering [12]. Table I summarizes the RMS Kullback-Leibler divergence computed over all fifty manually annotated links. Our divergence value is calculated using a Gaussian distribution assumption, compared to the human-labelled computed mean and variance.

We can see that overall, the UnLeSS-generated no-crossing state distribution has the lowest Kullback-Leibler divergence and hence is a better estimate of the distribution than using the ground-truth position and the elliptical model. For the crossing state, the UnLeSS-generated distribution is a better fit to the actual distribution that the model generated distribution. It is better or similar to the crossing state X-means generated distribution.

B. State Prediction

We used the generated mean and variance along with the other HMM parameters to compute the forward probability. Then, we compared the the forward probability to a threshold for each link l and channel $c \in C$ to estimate the state for each time t. We then evaluate how well the affected links detection module performs using either the Baum Welch-based training and forward probabilities or the X-means clustering by comparing the false positive rate and the false negative rate. We considered the model predicted crossing state as the positive event and the model predicted no-crossing state as the negative event.

For Deployment I, using the Baum Welch-based training and forward probabilities for affected links detection, the false positive rate is 0.032 while the false negative rate is 0.67. For Deployment I, using X-means clustering, the false positive rate and the false negative rate are 0.20 and 0.24 respectively. For Deployment II, using the Baum Welch-based training and forward probabilities for affected links detection, the false positive rate is 0.03 while the false negative rate is 0.77. For Deployment II, using X-means clustering, the false positive rate and the false negative rate are 0.30 and 0.43 respectively.

The X-means-based clustering outperforms the Baum Welch-based training and forward probabilities for affected links detection. The reason for that can be explained looking at Figure 4. We can see that while the modeled area of effect between two sensor nodes is a neatly shaped ellipse, the actual area of effect deviates from the ellipse shape resulting in areas where comparing to the model predicted state will lead to a false positive (FP) or false negative (FN) cases while in actuality comparing to the actual state, it should be considered true positive (TP) and true negative (TN) cases respectively.

To confirm that the UnLeSS training with forward probabilities for affected links detection do predict the actual state and for that reason deviate from the model predicted states, we plotted RSS for each link l and channel $c \in C$ and highlighted the crossing periods according to the ellipse model prediction and the UnLeSS training and forward probabilities prediction. Figure 2 shows a sample of these plots. We can see that the UnLeSS state prediction, while it deviates from the ellipse model prediction, can accurately predict the periods when the RSS changes indicating the presence of a person near the link line.

To show that the affected links at a particular time t correlate with the actual position of the tracked person, we plot the the links whose forward probability at a particular time t exceeds the threshold. Figure 6 displays these link lines for two times during the experiments. As shown, there exists a correlation between the affected links and the actual position of the person being tracked. An interesting remark about this figure is that some of the links close to the actual locations are not affected such as link $(12, 22)$ at time 201 and link $(15, 7)$ at time 42. This validates our argument that the area of effect for each link line is non-regularly shaped.

C. Tracking

The forward probabilities for each link l and channel $c \in C$ are used as the measurements input to the RTI module. Calculating forward probabilities introduces adds latency. If we do not wish to penalize the localization error simply for being a fraction of a second delayed, we should calculate the RMSE by shifting the estimates forward in time by a fixed delay τ and then comparing to the actual coordinates. We should test the performance across a range of τ within $[-2, 2]$ seconds to learn what the latency of the method is. We use a penalized RMSE (PRMSE) where a penalty (P) is added if a person is localized while there is actually no person in the area of interest or the other way around. For a range of τ between $[-2, 2]$ seconds, we add add an offset of τ to each time t in our deployment measurements time stamps. We get the shifted by offset actual coordinates (ac) and the estimated coordinates (ec) of the tracked person, we then compute the penalized RMSE (PRMSE), e_p, as follows:

$$e_p = \Big\{ \sum_{t \in \mathcal{A} \cap \mathcal{E}} \|z(t) - \hat{z}(t)\|^2 + \sum_{t \in \mathcal{A} \triangle \mathcal{E}} P \Big\}^{1/2} \qquad (2)$$

where $\mathcal{A}$ and $\mathcal{E}$ are the sets of times when a person is actually and estimated to be present, respectively; z and $\hat{z}(t)$ are the

actual and estimated coordinates of the person at time t; $\|\cdot\|$ indicates Euclidean distance; and $\cap$ and $\triangle$ indicate set union and set difference, respectively.

	Deploy I		Deply II	
	PRMSE (m)	Offset (s)	PRMSE (m)	Offset (s)
RTI	1.02	-0.75	0.66	-1.00
VRTI	2.39	-1.25	0.64	-1.75
FPRTI	0.66	-1.25	0.40	-1.25
CFPRTI	0.68	-1.25	0.52	-1.25
XFPRTI	0.76	-1.25	0.57	-1.50

TABLE II: Summarizes localization error for shadowing-based RTI (RTI), variance-based RTI (VRTI), forward probability-based RTI (FPRTI), combined channels forward probability-based RTI (CFPRTI) and X-means forward probability RTI (XFPRTI).

We evaluate the localization error for UnLeSS and compare it to other RTI-based localization techniques. UnLeSS uses forward probability-based RTI that calculates the forward probabilities for the trained HMMs at each time t for each link l and channel $c \in C$. It feeds the calculated forward probabilities into the RTI module as the measurements y. Figure 7 shows the radio tomographic image at to times resulting from the RTI module. The actual and the estimated positions of the tracked person are shown on the figure. Comparing this to Figure 6, which shows the affected link lines at the same time stamps, there is a correlation between the locations of the affected links and the actual position of the tracked person.

Our deployment results show that using forward probability-based RTI gives more accurate localization estimates than both shadowing-based RTI [17] and variance-based RTI [18]. However, the Baum-Welch-based training for each transmitter (TX), receiver (RX), channel (CH) link combination is time consuming and computationally expensive with a computational complexity of order $O(L * T)$ where T is the length of observations sequence and L is the number of links, $L = N(N-1)C$. Note $L = 3480$ for 30 sensors and four channels. Instead, we propose an alternative method in which we combine all channels for each TX/RX combination into one measurement. In this alternative, we average $2C$ channels' RSS measurements for each pair of devices, that is, for all C channels and for both directions of the link, e.g., where the first in the pair is the TX and second device is the RX, and vice versa. During the Baum Welch-based training, we use the product of the emission probabilities B of each channel $c \in C$ as the emission probability for the link line (Tx,Rx) assuming different channels measurements are independent. The computational complexity would, then, be reduced to $O(T * LogL)$.

To compare the effect of the unsupervised learning technique used on the localization error, we used X-means clustering to find the mean and variance for both the crossing and the no-crossing states. The calculated means and variances are used as the corresponding means and variances for the emission probability distributions for the HMMs in the affected links detection module while the π and A are initialized. Then, the forward probabilities are calculated and fed into the RTI module for localization.

Table II summarizes localization error for the shadowing-based RTI (RTI) [17], variance-based RTI (VRTI) [18], forward probability-based RTI (FPRTI), combined channels forward probability-based RTI (CFPRTI) and X-means forward probability RTI (XFPRTI). We found 35% minimum decrease of error comparing FPRTI to RTI and 37% minimum decrease of error comparing FPRTI to VRTI. FPRTI results in the least PRMSE, performing better that even the XFPRTI. Using CFPRTI has a tradeoff between a small localization accuracy degradation and less computational complexity.

VI. Related Work

Device-free localization has gained momentum in the past decade. There is a plethora of literature that explores different methodologies and deals with their challenges.

Researchers in [22] proposed a location determination system that does not require the presence of a physical device attached to the person being tracked or the tracked device to participate actively in the localization process. This is done by monitoring and processing changes in the received signal strength to detect changes in the environment corresponding to the existence of the person being tracked.

One approach for device-free localization is the use of RSS fingerprinting or radio maps. In such approach, the training phase is done by having a person standing at different predefined points and RSS measurements is recorded for each position. Then, when the system is in use, RSS measurements are collected and compared with the radio map and the estimated position is found by interpolating multiple best matching positions [16].

RSS fingerprinting makes use of the multipath effect as it leads to having different set of RSS measurements at differents human positions. However, such approach requires offline training and any change that happens to the environment i.e., furniture movement, will corrupt the training data and mandates another training.

Another approach for DFL is to estimate an image of the change in environment. The image can then be used to localize and track people within the environment using image processing techniques. This is called radio tomographic imaging (RTI) [18], [17], [10], [7].

The attenuation caused by each voxel is represented using measurements of RSS for each link in a wireless network. This methodology is referred to as shadowing-based RTI, since the measurements used to estimate the image measure shadowing loss. The generated images can be used to accurately track a person or more in the environment [17].

Another methodology for RTI is called variance-based RTI. In such approach, the windowed variance of RSS on each link is used as the measurement and the estimated image represents a quantification of the motion within each voxel [18].

Paper [19] presents another RTI-based methodology that is capable of detecting both stationary and moving entities unlike

pre-existing model-based methods for DFL which are unable to locate stationary people in heavily obstructed environments. The authors using extensive experimental data show that RSS measurements due to human movement can be modeled by the skew Laplace distribution whose parameters depend on the fade level, defined by the paper, and the location of the entity to be tracked whether it is on LOS or off LOS.

A different approach for DFL is presented in [24]. This paper proposes a system for tracking a moving person or object through walls using wireless networks making use of the motion-induced variation of received signal strength (RSS) measurements in a radio tomography network. It shows that RSS distribution on a wireless link can be modeled as a mixture of Gaussians, namely two Gaussians a foreground and a background. A foreground detection method is presented that allows tracking the coordinates of a moving person or object in different NLOS environments without changing system parameters. No offline training is required, so that system can be deployed rapidly.

Compared to fingerprinting DFL systems, the proposed system doesn't require tedious radio map collection. Compared to other RTI systems it enables high localization accuracy without parameter tuning or re-tuning after environmental changes.

VII. Conclusions

In this paper, we present Baum-Welch-based unsupervised learning, UnLeSS, to enhance the robustness of RSS-based DFL against environment changes and to learn the crossing/no-crossing distribution parameters. We present a HMM RTI system to detect the probability of a link line being in the crossing or the no-crossing state and hence increase the accuracy of localization. The performance of our system is validated in two different indoor environments. The results demonstrate that our UnLeSS outperforms a current RTI system and the combined X-means unsupervised learning with RTI. The results indicate that the presented system is capable of achieving less than 0.66 m localization accuracy. In future work, we will investigate the effect of environment changes on the system accuracy, the effect of having multiple persons in the area of interest to be tracked and expand our investigation to include more unsupervised learning techniques.

Acknowledgements

This material is based upon work supported by the US National Science Foundation under Grant #1407949. Neal Patwari is also affiliated with Xandem Technology LLC and Vita Sensors LLC.

References

[1] Maurizio Bocca, Ossi Kaltiokallio, and Neal Patwari. Radio tomographic imaging for ambient assisted living. In Stefano Chessa and Stefan Knauth, editors, *Evaluating AAL Systems Through Competitive Benchmarking*, volume 362 of *Communications in Computer and Information Science*, pages 108–130. Springer Berlin Heidelberg, 2013.

[2] Peter Hillyard, Anh Luong, and Neal Patwari. Highly reliable signal strength-based boundary crossing localization in outdoor time-varying environments. In *IEEE/ACM Information Processing in Sensor Networks (IPSN 2016)*, pages 1–12, April 2016.

[3] Texas Instruments. A usb-enabled system-on-chip solution for 2.4 ghz ieee 802.15.4 and zigbee applications. [online]. http://www.ti.com/lit/ds/symlink/cc2531.pdf.

[4] O. Kaltiokallio, M. Bocca, and N. Patwari. Enhancing the accuracy of radio tomographic imaging using channel diversity. In *Mobile Adhoc and Sensor Systems (MASS), 2012 IEEE 9th International Conference on*, pages 254–262, Oct 2012.

[5] Ossi Kaltiokallio, Maurizio Bocca, and Neal Patwari. Enhancing the accuracy of radio tomographic imaging using channel diversity. In *2012 IEEE 9th International Conference on Mobile Ad-Hoc and Sensor Systems (MASS 2012)*, pages 254–262. IEEE, 2012.

[6] Ossi Kaltiokallio, Maurizio Bocca, and Neal Patwari. A fade level-based spatial model for radio tomographic imaging. *IEEE Transactions on Mobile Computing*, Dec. 2013.

[7] Mohammad A Kanso and Michael G Rabbat. Compressed rf tomography for wireless sensor networks: Centralized and decentralized approaches. In *Distributed Computing in Sensor Systems*, pages 173–186. Springer, 2009.

[8] Brad Mager, Philip Lundrigan, and Neal Patwari. Fingerprint-based device-free localization performance in changing environments. *IEEE J. Sel. Areas in Communications*, 33(11):2429–2438, 2015.

[9] N Patwari and J Wilson. See through walls: Motion tracking using variance-based radio tomography networks,. *IEEE on transaction on mobile computing*, 2010.

[10] Neal Patwari and Piyush Agrawal. Effects of correlated shadowing: Connectivity, localization, and rf tomography. In *Information Processing in Sensor Networks, 2008. IPSN'08. International Conference on*, pages 82–93. IEEE, 2008.

[11] Neal Patwari and Joey Wilson. Rf sensor networks for device-free localization: Measurements, models, and algorithms. *Proceedings of the IEEE*, 98(11):1961–1973, 2010.

[12] Dan Pelleg, Andrew W Moore, et al. X-means: Extending k-means with efficient estimation of the number of clusters. In *ICML*, volume 1, 2000.

[13] Neal Patwari Peter Hillyard, Anh Luong. Highly reliable signal strength-based boundary crossing localization in outdoor time-varying environments. In *IPSN*, 2016.

[14] Lawrence R Rabiner. A tutorial on hidden markov models and selected applications in speech recognition. *Proceedings of the IEEE*, 77(2):257–286, 1989.

[15] Lawrence R Rabiner and Biing-Hwang Juang. An introduction to hidden markov models. *ASSP Magazine, IEEE*, 3(1):4–16, 1986.

[16] Moustafa Seifeldin, Ahmed Saeed, Ahmed E Kosba, Amr El-Keyi, and Moustafa Youssef. Nuzzer: A large-scale device-free passive localization system for wireless environments. *Mobile Computing, IEEE Transactions on*, 12(7):1321–1334, 2009.

[17] Joey Wilson and Neal Patwari. Radio tomographic imaging with wireless networks. *Mobile Computing, IEEE Transactions on*, 9(5):621–632, 2010.

[18] Joey Wilson and Neal Patwari. See-through walls: Motion tracking using variance-based radio tomography networks. *Mobile Computing, IEEE Transactions on*, 10(5):612–621, 2011.

[19] Joey Wilson and Neal Patwari. A fade-level skew-laplace signal strength model for device-free localization with wireless networks. *Mobile Computing, IEEE Transactions on*, 11(6):947–958, 2012.

[20] Chenren Xu, Bernhard Firner, Robert S Moore, Yanyong Zhang, Wade Trappe, Richard Howard, Feixiong Zhang, and Ning An. SCPL: Indoor device-free multi-subject counting and localization using radio signal strength. In *2013 ACM/IEEE Information Processing in Sensor Networks (IPSN)*, pages 79–90, April 2013.

[21] Hüseyin Yiğitler, Riku Jäntti, Ossi Kaltiokallio, and Neal Patwari. Detector based radio tomographic imaging. Technical Report arXiv:1604.03083 [cs.ET], arXiv.org, April 2016.

[22] Moustafa Youssef, Matthew Mah, and Ashok Agrawala. Challenges: device-free passive localization for wireless environments. In *Proceedings of the 13th annual ACM international conference on Mobile computing and networking*, pages 222–229. ACM, 2007.

[23] Dian Zhang, Jian Ma, Quanbin Chen, and Lionel M Ni. An rf-based system for tracking transceiver-free objects. In *Pervasive Computing and Communications, 2007. PerCom'07. Fifth Annual IEEE International Conference on*, pages 135–144. IEEE, 2007.

[24] Yi Zheng and Aidong Men. Through-wall tracking with radio tomography networks using foreground detection. In *Wireless Communications and Networking Conference (WCNC), 2012 IEEE*, pages 3278–3283. IEEE, 2012.